Pergamon

Polyhedron Vol. 14, No. 19, pp. 2803–2817, 1995
Elsevier Science Ltd
Printed in Great Britain
0277-5387/95 $9.50+0.00

0277-5387(95)00134-4

THE HETERONUCLEAR CLUSTER CHEMISTRY OF THE GROUP IB METALS—18.* SYNTHESIS, STRUCTURAL CHARACTERIZATION AND DYNAMIC BEHAVIOUR OF THE BIMETALLIC HEXANUCLEAR GROUP IB METAL CLUSTER COMPOUNDS $[M_2Ru_4H_2(\mu\text{-dppf})(CO)_{12}]$ [M = Cu, Ag or Au; dppf = $Fe(\eta^5\text{-}C_5H_4PPh_2)_2$]. X-RAY CRYSTAL STRUCTURE OF $[Cu_2Ru_4(\mu_3\text{-}H)_2(\mu\text{-dppf})(CO)_{12}]$†

IAN D. SALTER‡ and STEVEN A. WILLIAMS

Department of Chemistry, University of Exeter, Exeter EX4 4QD, U.K.

and

TRUSHAR ADATIA

School of Chemistry, University of North London, London N7 8DB, U.K.

Abstract—Treatment of a dichloromethane solution of the salt $[N(PPh_3)_2]_2[Ru_4(\mu\text{-}H)_2(CO)_{12}]$ with two equivalents of the complex $[M(NCMe)_4]PF_6$ (M = Cu or Ag) at −30°C, followed by the addition of one equivalent of 1,1′-bis(diphenylphosphino)ferrocene (dppf) affords the mixed-metal clusters $[M_2Ru_4(\mu_3\text{-}H)_2(\mu\text{-dppf})(CO)_{12}]$ [M = Cu (**1**) or Ag (**2**)] in *ca* 45–60% yield. The analogous gold-containing species $[Au_2Ru_4H_2(\mu\text{-dppf})(CO)_{12}]$ (**3**) was obtained in *ca* 70% yield by treating an acetone solution of $[N(PPh_3)_2]_2[Ru_4(\mu\text{-}H)_2(CO)_{12}]$ with a dichloromethane solution of the complex $[Au_2(\mu\text{-dppf})Cl_2]$, in the presence of $TlPF_6$. The novel cluster compounds **1**–**3** have been characterized by IR and NMR spectroscopy and the structure of **1** has been determined by a single-crystal X-ray diffraction study. The metal core structure of **1** consists of a tetrahedron of ruthenium atoms capped by a copper atom, with one of the $CuRu_2$ faces of the $CuRu_3$ tetrahedron so formed further capped by a second copper atom to give a capped trigonal bipyramidal skeletal geometry. The other two $CuRu_2$ faces of the $CuRu_3$ tetrahedron are each capped by a triply bridging hydrido ligand, the bidentate diphosphine ligand bridges the two coinage metals and each ruthenium atom is bonded to three terminal CO groups. The spectroscopic data of the silver- and gold-containing species **2** and **3** are closely similar to those of **1**, which suggests that **2** and **3** adopt similar metal core structures to that established for **1**. However, the possibility that the capped trigonal bipyramidal metal framework of **3** is distorted by the dppf ligand towards a capped square-based pyramidal skeletal geometry cannot be excluded with the evidence available. Variable-temperature ^1H and $^{31}P\{^1H\}$ NMR studies show that, at ambient temperatures in solution, the metal frameworks of all of the clusters undergo

* For Part 17, see ref. 1.

† This paper is dedicated to Prof. E. W. Abel on the occasion of his retirement from the Chair of Inorganic Chemistry at the University of Exeter. One of us (I. D. S.) is especially indebted to Eddie Abel for all of the advice, support and encouragement given to him while working at Exeter University. All of us would like to send our very best wishes to Prof. Abel for the future.

‡ Author to whom correspondence should be addressed.

dynamic behaviour involving coinage metal site exchange, even though the two Group IB metals are linked together by the bidentate diphosphine ligand dppf. Free energies of activation ($\Delta G^{\ddagger}$) at the coalescence temperature of 47 ± 1, 40 ± 1 and *ca* 33 kJ mol^{-1} have been calculated for the skeletal rearrangements from the coalescence temperatures observed in the variable-temperature $^{31}P\{^{1}H\}$ NMR spectra of clusters **1**, **2** and **3**, respectively. These values of $\Delta G^{\ddagger}$ are compared with those of structurally related analogous clusters. In addition, the dppf ligand attached to the coinage metals in each of **1**–**3** is also stereochemically non-rigid in solution at room temperature and it undergoes a process involving inversion of configuration at the phosphorus atoms, together with twisting of the cyclopentadienyl rings. The skeletal rearrangement process and the fluxional behaviour of the dppf ligand are definitely independent for clusters **2** and **3**.

Theoretical studies[2–4] of the bonding capabilities of $M(PR_3)$ (M = Cu, Ag or Au; R = alkyl or aryl) units suggest that the differences in energy between the various structural types can be very small for mixed-metal clusters which contain these fragments. This prediction is supported by experimental evidence,[5–8] which shows that Group IB metal heteronuclear clusters with very similar stoichiometries can exhibit markedly different metal core structures, skeletal isomerism can occur, both in solution and in the solid state, and the metal skeletons of this class of compound are often stereochemically non-rigid in solution.

Some of the earlier papers in this series[9–15] report the results of investigations into the chemistry of a selection of hexanuclear bimetallic clusters of general formula $[M_2Ru_4H_2(\mu\text{-}L_2)(CO)_{12}]$ (M = Cu, Ag or Au), in which the two Group IB metals are bridged by the bidentate ligands L_2 [$L_2 = Ph_2E(CH_2)_nE'PPh_2$ (E = E′ = P, n = 1–6; E = As, E′ = As or P, n = 1 or 2) or *cis*-$Ph_2PCH{=}CHPPh_2$]. It was found that the formal replacement of two PPh_3 groups attached to the gold atoms in $[Au_2Ru_4(\mu_3\text{-}H)(\mu\text{-}H)(CO)_{12}(PPh_3)_2]$ by $Ph_2E\text{-}CH_2E'Ph_2$ (E = As, E′ = As or P; E = E′ = P) or *cis*-$Ph_2PCH{=}CHPPh_2$ ligands causes the capped trigonal bipyramidal metal framework structure observed for the PPh_3-containing cluster to change to a capped square-based pyramidal skeletal geometry in each case.[9–12] The analogous cluster in which the two gold atoms are linked by the bidentate diphosphine $Ph_2P(CH_2)_2PPh_2$ adopts a metal core structure similar to the capped trigonal bipyramidal skeletal geometry of the PPh_3-containing cluster, but one of the Au—Ru distances is too long [3.446(4) Å] for any significant bonding interaction between the two atoms.[9] Thus, the metal framework structure of the cluster is somewhat distorted towards a capped square-based pyramidal geometry by the $Ph_2P(CH_2)_2PPh_2$ ligand.

In marked contrast, the clusters $[M_2Ru_4H_2(\mu\text{-}L_2)(CO)_{12}]$ [M = Cu or Ag, $L_2 = Ph_2E(CH_2)_nE'Ph_2$ (E = E′ = P, n = 1–6, E = As, E′ = As or P, n = 1 or 2) or *cis*-$Ph_2PCH{=}CHPPh_2$] and $[Au_2Ru_4H_2(\mu\text{-}L_2)(CO)_{12}]$ [$L_2 = Ph_2P(CH_2)_nPPh_2$ (n = 3–6)] all adopt capped trigonal bipyramidal metal framework structures in which the Group IB metals occupy two distinct sites.[9,11,13–15] Variable-temperature $^{31}P\{^{1}H\}$ and ^{1}H NMR spectroscopic studies have shown that each cluster undergoes dynamic behaviour in solution at room temperature. This stereochemical non-rigidity involves an intramolecular rearrangement of the cluster's metal skeleton in which the coinage metals exchange between the two distinct sites and the process occurs even though the two Group IB metals are linked together by a bidentate ligand in each cluster.[9,11,13–15] Changes in the nature of the bidentate ligands attached to the coinage metals have been found to cause relatively large alterations of up to *ca* 13 and *ca* 10 kJ mol^{-1} in the observed values of the free energy of activation ($\Delta G^{\ddagger}$) for the intramolecular metal core rearrangements in the copper- and silver-containing species, respectively.[11]

In view of the interesting results outlined above, we wished to extend the study to analogous clusters in which the Group IB metals are ligated by the bidentate diphosphine 1,1′-bis(diphenylphosphino)ferrocene (dppf). In particular, we were interested to determine the effect of the dppf ligand on the metal core structures and stereochemical non-rigidity of the mixed-metal clusters $[M_2Ru_4H_2(\mu\text{-dppf})(CO)_{12}]$ (M = Cu, Ag or Au). Additionally, single-crystal X-ray diffraction studies of cluster compounds containing a dppf ligand bridging two metal atoms are still relatively rare.[16,17]

RESULTS AND DISCUSSION

Synthesis of the clusters $[M_2Ru_4H_2(\mu\text{-dppf})(CO)_{12}]$ [M = Cu, Ag *or* Au; dppf = $(\eta^5\text{-}C_5H_4PPh_2)_2Fe$]

Treatment of a dichloromethane solution of the salt $[N(PPh_3)_2]_2[Ru_4(\mu\text{-}H)_2(CO)_{12}]$ with two equi-

Table 1. Analytical[a] and physical data for the new Group IB metal heteronuclear cluster compounds

Cluster compound	ν_{max}(CO)[b] (cm^{-1})	Yield (%)[c]	M.p. (θ/°C) (decomp.)	Analysis (%) C	H
1 $[Cu_2Ru_4(\mu_3\text{-}H)_2(\mu\text{-dppf})(CO)_{12}]$	2072 s, 2035 vs, 2019 vs, 2006 s, 1976 m(br), 1934 m(br)	60	129–134	38.5 (38.8)	2.4 (2.1)
2 $[Ag_2Ru_4(\mu_3\text{-}H)_2(\mu\text{-dppf})(CO)_{12}]$	2069 s, 2032 vs, 2018 vs, 2003 s, 1971 m(br), 1930 m(br)	46	175–178	36.6 (36.5)	2.0 (2.0)
3 $[Au_2Ru_4H_2(\mu\text{-dppf})(CO)_{12}]$	2070 s, 2053 m, 2035 s, 2020 vs, 1987 m(br), 1944 m(br)	68	135–140	32.7 (32.6)	1.9 (1.8)

[a] Calculated values given in parentheses.
[b] Measured in dichloromethane solution.
[c] Based on ruthenium reactant.

valents of the complex $[M(NCMe)_4]PF_6$ (M = Cu or Ag) at −30°C and the subsequent addition of one equivalent of dppf affords the dark red cluster compounds $[M_2Ru_4(\mu_3\text{-}H)_2(\mu\text{-dppf})(CO)_{12}]$ [M = Cu (**1**) or Ag (**2**)] in *ca* 45–60% yield. The analogous gold-containing cluster $[Au_2Ru_4H_2(\mu\text{-dppf})(CO)_{12}]$ (**3**) was prepared in *ca* 70% yield from the reaction of an acetone solution of $[N(PPh_3)_2]_2[Ru_4(\mu\text{-}H)_2(CO)_{12}]$ with a dichloromethane solution containing one equivalent of the compound $[Au_2(\mu\text{-dppf})Cl_2]$*, in the presence of $TlPF_6$. The clusters **1**–**3** were characterized by microanalysis and by spectroscopic measurements (Tables 1 and 2). The IR spectra of **1**–**3** closely resemble those reported[18] for the analogous species $[M_2Ru_4H_2(CO)_{12}(PPh_3)_2]$ (M = Cu, Ag or Au), implying that **1**–**3** adopt similar capped trigonal bipyramidal metal core structures to those observed for the PPh_3-containing clusters. The NMR spectroscopic data and microanalyses are fully consistent with the proposed formulations for **1**–**3**, but to investigate the structure of one cluster from the series in detail, a single-crystal X-ray diffraction study was performed on **1**. Discussion of the variable-temperature NMR spectra of **1**–**3** is best deferred until the X-ray diffraction results have been described.

X-ray crystal structure of $[Cu_2Ru_4(\mu_3\text{-}H)_2(\mu\text{-dppf})(CO)_{12}]$ (**1**)

The molecular structure of **1** is shown in Fig. 1, together with the crystallographic numbering scheme. Selected bond lengths and angles are summarized in Table 3. The X-ray diffraction study confirms that **1** adopts a capped trigonal bipyramidal skeletal geometry. The four ruthenium atoms form a tetrahedron, with one Ru_3 face [Ru(1)Ru(2)Ru(3)] capped by a copper atom [Cu(1)] and the Cu(1)Ru(2)Ru(3) face of the $CuRu_3$ tetrahedron so formed further capped by a second copper atom. The dppf ligand is attached to the two copper atoms and both the Cu(1)Ru(1)Ru(2) and Cu(1)Ru(1)Ru(3) faces of the metal skeleton are capped by a triply bridging hydrido ligand. Each ruthenium atom is bonded to three essentially linear carbonyl groups.

Figure 2 compares the values of the metal–metal separations in the framework of **1** with the equivalent distances in the metal cores of the closely related analogous clusters $[Cu_2Ru_4(\mu_3\text{-}H)_2\{\mu\text{-}Ph_2P(CH_2)_nPPh_2\}(CO)_{12}]$ [n = 2 (**4**), 3 (**5**) or 5 (**6**)],[13] in which the two copper atoms are also bridged by bidentate diphosphine ligands. The Cu—Ru distances measured for **1** are slightly larger in range than those observed in clusters **4**–**6**. However, the mean Cu—Ru separation of 2.724(2) Å in **1** is longer than the mean for **4** [2.685(2) Å]† and similar in magnitude to those in **5** [2.711(1) Å] and **6** [2.730(1) Å]. In each structure, the Cu(1)—Ru(1) and Cu(2)—Ru(2) distances are markedly longer than the remaining Cu—Ru separations. The longer Cu—Ru vectors are bridged by the hydrido ligands, which often lengthen the metal–metal bonds that they bridge. The range of Ru—Ru distances observed in the metal core of **1** is similar to those in **4** and **5**, but it is smaller than the range reported for **6**. The mean Ru—Ru separation in **1** [2.873(2) Å] is similar to that in **6** [2.870(1) Å], but it is larger than the mean values in **4** [2.868(2)]† and **5** [2.867(2) Å]. As observed for the Cu—Ru distances, the lengths of Ru(1)—Ru(2)

* Prepared *in situ* by treating a dichloromethane solution containing two equivalents of $[AuCl(SC_4H_8)]$ with one equivalent of dppf.

† Mean value of the metal–metal bonds of the two independent molecules in the asymmetric unit of **4**.[13]

Table 2. ^{1}H and ^{31}P NMR spectroscopic data[a] for the new Group IB metal heteronuclear cluster compounds

Cluster	Temperature (°C)	^{1}H NMR data[b]	$^{31}P\{^{1}H\}$ NMR data[c]
1	+22	−17.46 [t, br, 2H, μ_3-H, J(PH) = 6], 4.29 (s, br, 4H, C_5H_4), 4.62 (s, br, 4H, C_5H_4), 7.47–7.56 (m, 20, Ph)	−1.2 (s, vbr)
	−80	−17.76 [d, 1H, μ_3-H, J(PH) = 11], −17.51 [d, 1H, μ_3-H, J(PH) = 12], 3.88, 4.04, 4.32, 4.37, 4.44, 4.53, 5.02, 5.31 (8 × s, 1H each, C_5H_4), 7.11–8.04 (m, 20H, Ph)	1.8 (s, 1P), −4.6 (s, 1P)
2	+22	−17.23 [apparent t of t of t, 2H, μ_3-H, $J(^{109}AgH)$ = 15, $J(^{107}AgH)$ = 13, J(PH) = 5], 4.07 (s, br, 4H, C_5H_4), 4.56 (s, br, 4H, C_5H_4), 7.48–7.49 (m, 20H, Ph)	9.8 (m)[d]
	−60	−17.55 (s, vbr, 2H, μ_3-H), 3.61 (s, br, 2H, C_5H_4), 4.07 (s, 2H, C_5H_4), 4.43 (s, 2H, C_5H_4), 5.02 (s, br, 2H, C_5H_4), 7.18–7.78 (m, 20H, Ph)	—
	−90	—	12.1 [2 × d, br, 1P, $^{1}J(^{109}AgP)$ = 585, $^{1}J(^{107}AgP)$ = 501], 7.4 [2 × d of d, 1P, $^{1}J(^{109}AgP)$ = 479, $^{1}J(^{107}AgP)$ = 417, $^{2}J(AgP)_{av.}$ = 10]
	−100	−17.80 [d of d, 1H, μ_3-H, $J(AgH)_{av.}$ = 32, J(PH) = 10], −17.26 [d of d, 1H, μ_3-H, $J(AgH)_{av.}$ = 31, J(PH) = 9], 3.28, 3.66, 3.92, 4.07, 4.33, 4.36, 4.73, 5.06 (8 × s, 1H each, C_5H_4), 7.14–7.92 (m, 20H, Ph)	—
3	+22	−15.30 [t, 2H, hydrido H, J(PH) = 8], 4.09 (s, br, 4H, C_5H_4), 4.60 (s, br, 4H, C_5H_4), 7.43–7.58 (m, 20H, Ph)	53.6 (s)
	−60	−15.22 [t, 2H, hydrido H, J(PH) = 10], 3.61, 4.07, 4.45, 5.11 (4 × s, 2H each, C_5H_4), 7.21–7.80 (m, 20H, Ph)	—
	−100	*ca* −15.4 (s, vbr, 2H, hydrido H), *ca* 3.6, (s, vbr, 2H, C_5H_4), *ca* 4.1 (s, vbr, 2H, C_5H_4), 4.47 (s, br, 2H, C_5H_4), *ca* 5.1 (s, vbr, 2H, C_5H_4), 7.22–7.82 (m, 20H, Ph)	*ca* 58 (s, vbr), *ca* 39 (s, vbr)[e]

[a] Chemical shifts (δ) in ppm, coupling constants in Hz.

[b] Measured in dichloromethane-d_2 solution.

[c] ^{1}H decoupled, measured in dichloromethane-d_2–CH_2Cl_2 solution. Chemical shifts positive to high frequency of 85% aqueous H_3PO_4 (external).

[d] The multiplet consists of superimposed subspectra due to the $^{107}Ag^{107}Ag$, $^{107}Ag^{109}Ag$ and $^{109}Ag^{109}Ag$ isotopomers of the cluster and it is complicated by second-order effects and by a wide variety of silver–silver and silver–phosphorus couplings. The observed pattern of signals for **2** is very similar to those reported previously[14] in the ambient-temperature $^{31}P\{^{1}H\}$ NMR spectra of the clusters $[Ag_2Ru_4(\mu_3\text{-}H)_2\{\mu\text{-}Ph_2P(CH_2)_nPPh_2\}(CO)_{12}]$ (n = 4 or 5), which are structurally closely related to **2**. Analysis of the spectra of the two $Ph_2P(CH_2)_nPPh_2$-containing clusters has demonstrated that the observed multiplet signals are consistent with a single averaged environment for the pair of phosphorus atoms and a single averaged environment for the pair of silver atoms.[14] Although it is possible to obtain the values of the coupling constants $^{1}J(^{109}AgP)$, $^{1}J(^{107}AgP)$, $^{2}J(^{109}AgP)$, $^{2}J(^{107}AgP)$, $J(^{109}Ag^{109}Ag)$, $J(^{109}Ag^{107}Ag)$ and $J(^{107}Ag^{107}Ag)$ from computer simulations of the observed multiplet signals,[14] it was not considered worthwhile to do so for **2**.

[e] The two observed singlets are far too broad to permit accurate integration.

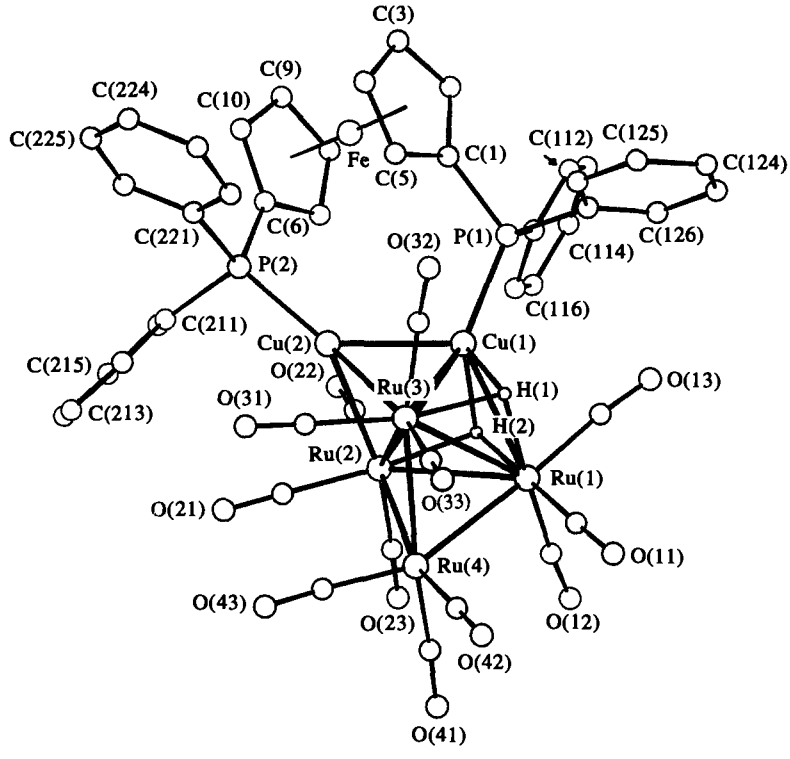

Fig. 1. Molecular structure of $[Cu_2Ru_4(\mu_3\text{-}H)_2(\mu\text{-dppf})(CO)_{12}]$ (**1**), showing the crystallographic numbering. The carbon atom of each carbonyl group has the same number as the oxygen atom.

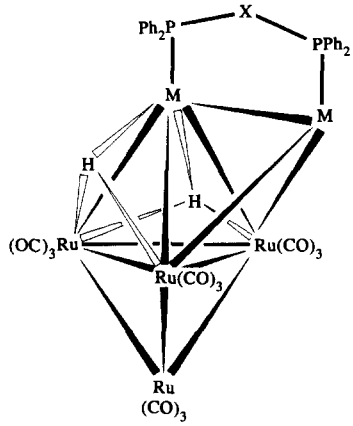

	M	X
(1)	Cu	Fe $(\eta^5\text{-}C_5H_4)_2$
(2)	Ag	Fe $(\eta^5\text{-}C_5H_4)_2$
(3)	Au	Fe $(\eta^5\text{-}C_5H_4)_2$
(4)	Cu	$(CH_2)_2$
(5)	Cu	$(CH_2)_3$
(6)	Cu	$(CH_2)_5$

and Ru(1)—Ru(3), which are bridged by the hydrido ligands, are noticeably longer than the remaining Ru—Ru distances in each structure. As expected,[13] the lengths of the three unbridged Ru—Ru vectors [Ru(1)—Ru(4), Ru(2)—Ru(4) and Ru(3)—Ru(4)] in the Ru_4 tetrahedron of **1** and **4**–**6** are altered very little by changes in the bidentate diphosphine ligand. The difference in the nature of the attached phosphine ligand between **1** and **4**–**6** also causes relatively small variations in the lengths of the Ru—Ru vectors bridged by the hydrido ligands and/or the copper atoms [Ru(1)—Ru(2), Ru(1)—Ru(3) and Ru(2)—Ru(3)], as observed previously for **4**–**6**.[13] However, the "softness" of the bonding between the Group IB metals themselves and between coinage metals and other transition metals is well established[6–9,13] and significant differences are observed in the magnitudes of the Cu—Cu separation and the equivalent individual Cu—Ru distances when **1** is compared with **4**–**6**. The Cu—Cu vector in **1** [2.528(2) Å] is intermediate in length between those in **4** and **5**. However, the size of the Cu(1)—Ru(1) separation [2.777 (2) Å] is closely similar to that in **6**, whereas the values of the Cu(1)—Ru(2) [2.830 (2) Å] and Cu(1)—Ru(3) [2.713 (2) Å] distances are much nearer to those observed for **4**. The Cu(2)—Ru(2) [2.663(2) Å] and Cu(2)—Ru(3) [2.637(2) Å] vectors, which are not bridged by hydrido ligands, have magnitudes most closely similar to those in **5**.

The dppf ligand bridges the two copper atoms with the ferrocenyl unit positioned directly over the mid-point of the Cu—Cu vector and the iron atom lying on a pseudo-C_2 axis, which also passes through the midpoint of the Cu—Cu vector (Fig. 3). The two cyclopentadienyl rings of the ferrocenyl

Table 3. Selected bond lengths (Å) and angles (°), with estimated standard deviations in parentheses, for $[Cu_2Ru_4(\mu_3\text{-}H)_2(\mu\text{-dppf})(CO)_{12}]$ (**1**)

Ru(1)—Ru(2)	2.940(1)	Ru(1)—Ru(3)	2.986(1)
Ru(1)—Ru(4)	2.782(2)	Ru(1)—Cu(1)	2.777(2)
Ru(2)—Ru(3)	2.907(1)	Ru(2)—Ru(4)	2.812(2)
Ru(2)—Cu(1)	2.830(2)	Ru(2)—Cu(2)	2.663(2)
Ru(3)—Ru(4)	2.808(2)	Ru(3)—Cu(1)	2.713(2)
Ru(3)—Cu(2)	2.637(2)	Cu(1)—Cu(2)	2.528(2)
Cu(1)—P(1)	2.237(4)	Cu(2)—P(2)	2.224(4)
Range of Fe—C(Cp)	2.020(8)–2.082(8)		
Range of Ru—CO	1.843(18)–1.898(14)		
Range of C—O	1.147(20)–1.200(18)		

Ru(3)—Ru(1)—Ru(2)	58.7(1)	Ru(4)—Ru(1)—Ru(2)	58.8(1)
Ru(4)—Ru(1)—Ru(3)	58.1(1)	Cu(1)—Ru(1)—Ru(2)	59.3(1)
Cu(1)—Ru(1)—Ru(3)	56.0(1)	Cu(1)—Ru(1)—Ru(4)	105.2(1)
Ru(3)—Ru(2)—Ru(1)	61.4(1)	Ru(4)—Ru(2)—Ru(1)	57.8(1)
Ru(4)—Ru(2)—Ru(3)	58.8(1)	Cu(1)—Ru(2)—Ru(1)	57.5(1)
Cu(1)—Ru(2)—Ru(3)	56.4(1)	Cu(1)—Ru(2)—Ru(4)	103.0(1)
Cu(2)—Ru(2)—Ru(1)	104.6(1)	Cu(2)—Ru(2)—Ru(3)	56.3(1)
Cu(2)—Ru(2)—Ru(4)	111.6(1)	Cu(2)—Ru(2)—Cu(1)	54.7(1)
Ru(2)—Ru(3)—Ru(1)	59.8(1)	Ru(4)—Ru(3)—Ru(1)	57.3(1)
Ru(4)—Ru(3)—Ru(2)	58.9(1)	Cu(1)—Ru(3)—Ru(1)	58.1(1)
Cu(1)—Ru(3)—Ru(2)	60.4(1)	Cu(1)—Ru(3)—Ru(4)	106.2(1)
Cu(2)—Ru(3)—Ru(1)	104.0(1)	Cu(2)—Ru(3)—Ru(2)	57.2(1)
Cu(2)—Ru(3)—Ru(4)	112.6(1)	Cu(2)—Ru(3)—Cu(1)	56.4(1)
Ru(2)—Ru(4)—Ru(1)	63.4(1)	Ru(3)—Ru(4)—Ru(1)	64.6(1)
Ru(3)—Ru(4)—Ru(2)	62.3(1)	Ru(2)—Cu(1)—Ru(1)	63.2(1)
Ru(3)—Cu(1)—Ru(1)	65.9(1)	Ru(3)—Cu(1)—Ru(2)	63.2(1)
Cu(2)—Cu(1)—Ru(1)	113.4(1)	Cu(2)—Cu(1)—Ru(2)	59.3(1)
Cu(2)—Cu(1)—Ru(3)	60.3(1)	P(1)—Cu(1)—Ru(1)	133.2(1)
P(1)—Cu(1)—Ru(2)	148.5(1)	P(1)—Cu(1)—Ru(3)	143.7(1)
P(1)—Cu(1)—Cu(2)	113.4(1)	Ru(3)—Cu(2)—Ru(2)	66.5(1)
Cu(1)—Cu(2)—Ru(2)	66.0(1)	Cu(1)—Cu(2)—Ru(3)	63.4(1)
P(2)—Cu(2)—Ru(2)	137.0(1)	P(2)—Cu(2)—Ru(3)	151.6(1)
P(2)—Cu(2)—Cu(1)	134.2(1)		
Range of Ru—C—O	169(1)–176(1)		

unit are tilted by 0.35° from being co-parallel and they deviate by 8° from being eclipsed. Although the two C_5 rings are locked in an approximately eclipsed orientation, the rings are mutually twisted so that the two C—P vectors deviate from one another by 80°. Similar twisting of the cyclopentadienyl rings has also been observed in the dppf-containing cluster compounds $[Ru_3(\mu\text{-dppf})(CO)_{10}]$[17] and $[Au_2Ru_4(\mu\text{-dppf})(CO)_{12}BH]$.[16] It has been suggested previously that twisting and/or tilting of the C_5 rings are possible ways in which the dppf ligand can modify its conformation to address any steric constraints that are imposed when the ligand chelates to metal atoms.[19] Twisting of the two M—P vectors relative to each other to minimize steric strain has also been observed in other clusters in which a bidentate diphosphine ligand bridges two Group IB metals (M).[13,14] To some extent, this degree of flexibility within the bidentate ligand is governed by the type of backbone which holds the two phosphorus atoms together. It is of interest to compare the dihedral angle between the two Cu—P vectors in **1** with those observed for the closely related analogous clusters **4**–**6**.[13] The dihedral angle in **1** (12.4°), in which the two phosphorus atoms are held together by the ferrocenyl unit, is smaller than that in **4** (12.9°), where the two phosphorus atoms are linked by two —CH_2— units, and it is markedly smaller than those in **5** (13.6°) and **6** (14.8°), where three and five methylene units bridge the two phosphorus atoms, respectively. Clearly, the longer aliphatic backbones in **5** and **6** allow more flexibility within the bidentate diphosphine ligand than the ferrocenyl unit does in **1**.

Unusually short M···C contacts between the

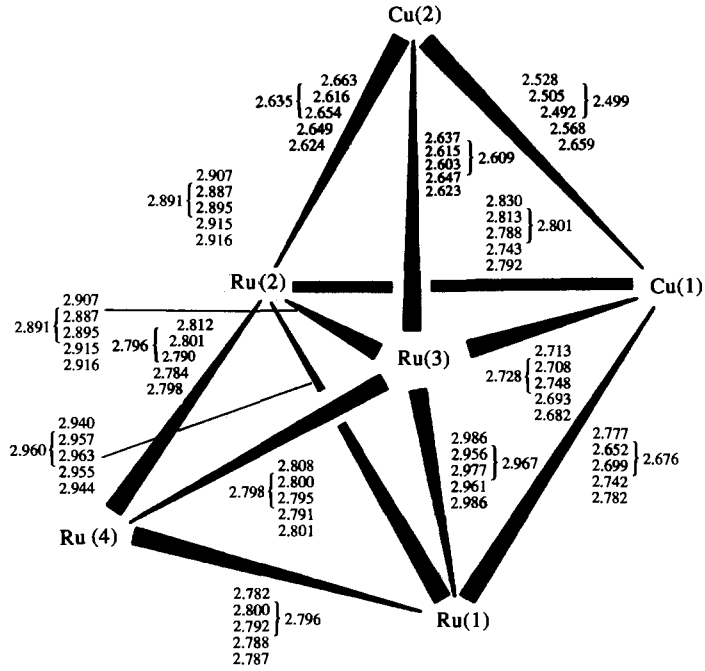

Fig. 2. A comparison of the metal–metal separations (Å) in the metal frameworks of $[Cu_2Ru_4(\mu_3\text{-}H)_2(\mu\text{-}L_2)(CO)_{12}]$ [L_2 = dppf (**1**) or $Ph_2P(CH_2)_nPPh_2$ {n = 2 (**4**), 3 (**5**) or 5 (**6**)}]. [There are two independent molecules (A and B) in the asymmetric unit of **4**.[13]] Distances are given in the following descending order: **1**, molecule A of **4**,[13] molecule B of **4**,[13] **5**[13] and **6**.[13] The single figures adjacent to the brackets are the mean averages of the equivalent separations in molecules A and B of **4**.

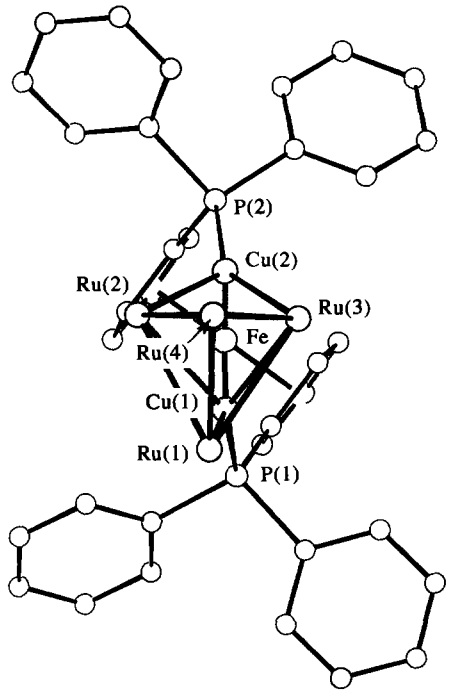

Fig. 3. The relative orientation of the dppf ligand and the metal skeleton of $[Cu_2Ru_4(\mu_3\text{-}H)_2(\mu\text{-dppf})(CO)_{12}]$ (**1**), showing how the dppf ligand removes the plane of symmetry through Cu(1), Cu(2), Ru(1) and Ru(4) in the ground-state metal core structure of **1**. The hydrido and carbonyl ligands have been omitted for clarity.

coinage metals (M) and essentially linear carbonyl ligands bonded to adjacent metals are often observed in the solid-state structures of Group IB metal heteronuclear clusters.[6,8] Compound **1** also exhibits this structural feature, with the Cu(2)···C(31) distance being only 2.616(15) Å. However, despite the fact that this type of short M···C contact frequently occurs, the exact nature of the interaction is not well understood.[6,8] It is not clear whether the contacts represent some degree of long range interaction, either attractive[20–23] or repulsive,[24] between the coinage metals and the carbonyl ligands, or result from steric effects in the solid.[25] A combination of incipient Ag···CO bonding and intramolecular steric pressure between oxygen atoms of carbonyl ligands has also been suggested as an explanation in the case of a silver-containing heteronuclear cluster.[26] However, studies on some gold-containing systems have indicated that there are no significant bonding interactions involved in the short Au···C contacts observed for these compounds.[27]

Variable-temperature NMR spectroscopic studies and dynamic behaviour of the clusters $[M_2Ru_4H_2(\mu\text{-dppf})(CO)_{12}]$ (M = Cu, Ag *or* Au)

Having established the molecular structure of **1**, it is now possible to interpret the variable-tem-

perature ^1H and $^{31}P\{^1H\}$ NMR spectra of **1–3** (Table 2). The low-temperature ^1H and $^{31}P\{^1H\}$ NMR spectra obtained for **1** are completely consistent with the ground-state structure determined by the X-ray diffraction study, and those observed for **2** and **3** strongly suggest that **2** and **3** adopt closely similar structures. However, the possibility that the capped trigonal bipyramidal metal framework of the gold-containing cluster **3** is distorted by the dppf ligand towards a capped square-based pyramidal skeletal geometry cannot be excluded with the evidence available. The bidentate diphosphine ligand $Ph_2P(CH_2)_2PPh_2$ is known[9] to cause a distortion of this type for the metal framework of the cluster $[Au_2Ru_4(\mu_3\text{-}H)(\mu\text{-}H)\{\mu\text{-}Ph_2P(CH_2)_2PPh_2\}(CO)_{12}]$, which is closely related to **3**. Also, it is not possible to determine unambiguously whether the two hydrido ligands in **3** are both face-capping or whether one is face-capping and one is edge-bridging (see below).

At −90°C, the $^{31}P\{^1H\}$ NMR spectra of **1** and **2** each show two phosphorus resonances of equal intensity, which is consistent with the two distinct Group IB metal sites in the capped trigonal bipyramidal ground-state metal core structures of the clusters [e.g. Cu(1) and Cu(2) in Fig. 2]. The two phosphorus signals visible in the spectrum of the silver-containing cluster **2** are each split into two doublets by ^{107}Ag–^{31}P and ^{109}Ag–^{31}P couplings through one bond, and one of them is also further split into two doublets of doublets by a small $^{107,109}Ag$–^{31}P coupling* through two bonds. The other phosphorus signal is slightly broadened at −90°C, so the expected[13] small $^{107,109}Ag$–^{31}P coupling through two bonds cannot be resolved. Two phosphorus resonances are also visible in the $^{31}P\{^1H\}$ NMR spectrum of the gold-containing cluster **3** at −100°C, but the peaks are severely broadened by the dynamic behaviour of the cluster (see below). As the temperature is raised from −90 or −100°C, the two separate phosphorus signals in the $^{31}P\{^1H\}$ NMR spectrum of each of the clusters **1–3** broaden and then coalesce. At ambient temperatures, a singlet is observed in the $^{31}P\{^1H\}$ NMR spectrum of each of **1** and **3**. In the case of **1**, the peak is broadened by quadrupolar effects from the copper atoms.[13,18,28–30] The pattern of peaks observed in the ambient-temperature $^{31}P\{^1H\}$ NMR spectrum of the silver-containing cluster **2** is very similar to the multiplets reported previously[14] for the analogous clusters $[Ag_2Ru_4(\mu_3\text{-}H)_2\{\mu\text{-}Ph_2P(CH_2)_nPPh_2\}(CO)_{12}]$ ($n = 4$ or 5), which are structurally related to **2**. Analysis of the spectra of the two $Ph_2P(CH_2)_nPPh_2$-containing clusters has demonstrated that the observed multiplet signals are consistent with a single averaged environment for the pair of phosphorus atoms and a single averaged environment for the pair of silver atoms.[14] The multiplets actually consist of superimposed subspectra due to the $^{107}Ag^{107}Ag$, $^{107}Ag^{109}Ag$ and $^{109}Ag^{109}Ag$ isotopomers of the clusters and they are complicated by second-order effects and by silver–phosphorus couplings through one and two bonds and silver–silver couplings.[14] Thus, the variable-temperature $^{31}P\{^1H\}$ NMR data clearly demonstrate that, at ambient temperature in solution, each of the clusters **1–3** undergoes dynamic behaviour which exchanges the phosphorus atoms between the two distinct sites in the ground-state structures.

Similar NMR spectroscopic results to those obtained for **1–3** have previously been observed for a series of analogous clusters with capped trigonal bipyramidal M_2Ru_4 metal skeletons, and it has been shown that an intramolecular rearrangement of the actual metal framework of the cluster, together with a concomitant site-exchange process for the two hydrido ligands, is the only reasonable explanation for them.[9,11,13–15,18] The two coinage metals exchange between the two distinct sites in the ground-state metal framework structure and they simultaneously move the attached phosphorus atoms. This dynamic process has actually been observed directly by $^{109}Ag\{^1H\}$ INEPT NMR spectroscopy for $[Ag_2Ru_4(\mu_3\text{-}H)_2\{\mu\text{-}Ph_2E(CH_2)_nEPh_2\}(CO)_{12}]$ (E = P, $n = 1$, 2 or 4; E = As, $n = 1$).[14,15] Therefore, to explain the observed $^{31}P\{^1H\}$ NMR spectra, we propose that the two Group IB metals in each of the novel clusters **1–3** undergo intramolecular site-exchange at ambient temperature in solution, even though they are linked together by the dppf ligand (Fig. 4a).

The coalescence temperatures for the intramolecular metal core rearrangements of **1–3** can be measured from the variable-temperature $^{31}P\{^1H\}$ NMR spectra. For **1** and **2**, the observed coalescence temperatures of 258 ± 5 and 218 ± 5 K give values of the free energy of activation at the coalescence temperature ($\Delta G^{\ddagger}$) for the skeletal rearrangement of 47 ± 1 and 40 ± 1 kJ mol^{-1}, respectively. It was not possible to obtain very good quality low-temperature spectra for **3**, because of its poor solubility in all organic solvents, but the coalescence temperature can be estimated as *ca* 193 K, which corresponds to a value of $\Delta G^{\ddagger}$ at the coalescence temperature of *ca* 33 kJ mol^{-1}. Thus, the magnitude of $\Delta G^{\ddagger}$ for the intramolecular metal core rearrange-

* The magnitude of the coupling through two bonds is not sufficiently large to allow the two separate contributions from ^{107}Ag and ^{109}Ag to be resolved.

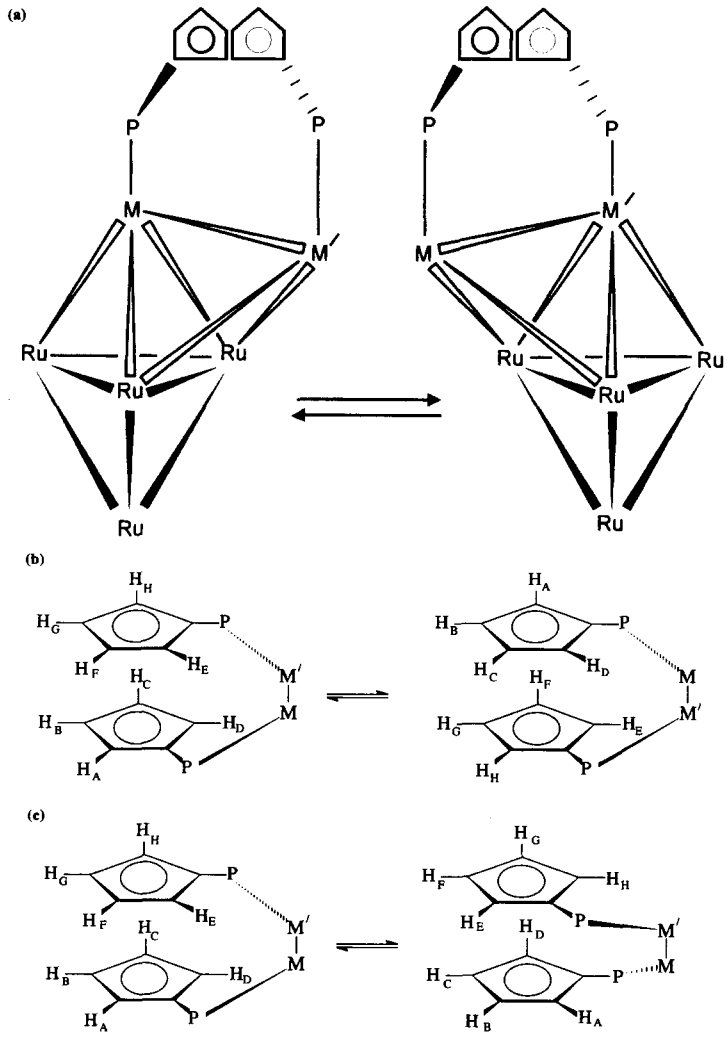

Fig. 4. Schematic representations of the two dynamic processes which the clusters $[M_2Ru_4H_2(\mu\text{-dppf})(CO)_{12}]$ [M = Cu (**1**), Ag (**2**) or Au (**3**)] undergo in solution. In each case, the iron atom and the phenyl rings of the dppf ligand have been omitted for clarity. (a) The intramolecular metal core rearrangement, which exchanges the two coinage metals (M and M′) in each of **1–3** between the two distinct sites [e.g. Cu(**1**) and Cu(**2**) in Fig. 2] in the capped trigonal bipyramidal metal skeletons of the clusters, shown when the dppf ligand is stereochemically rigid. (b) The effect of the intramolecular metal core rearrangement on the Cp hydrogens when the dppf ligand is stereochemically rigid. (c) The inversion of configuration at the phosphorus atoms and twisting of the Cp rings observed for the dppf ligand. At the low-temperature limit, Cp hydrogens H_A–H_H are all inequivalent (Fig. 6), so eight signals are observed in the ^1H NMR spectra of **1** and **2** (e.g. Fig. 5). However, at intermediate temperatures, the skeletal rearrangements of **2** and **3** are fast on the NMR timescale, but the dppf ligand fluxional process cannot be observed. Thus, the site-exchange of Group IB metals M and M′ also causes exchange to occur between the following pairs of Cp hydrogens, $H_A \leftrightarrow H_H$, $H_B \leftrightarrow H_G$, $H_C \leftrightarrow H_F$ and $H_D \leftrightarrow H_E$, and four Cp peaks are observed in the ^1H NMR spectra of **2** (Fig. 5) and **3** at −60 or −50°C. At the high-temperature limit, both the metal core rearrangement and the dppf ligand fluxion are fast on the NMR timescale. The latter dynamic process produces effective mirror planes through both of the two C_5H_4P units of the dppf ligand and exchanges the pairs of protons $H_A \leftrightarrow H_D$, $H_B \leftrightarrow H_C$, $H_E \leftrightarrow H_H$ and $H_F \leftrightarrow H_G$. Therefore, the combination of the two fluxional processes renders the set of four hydrogens H_A, H_D, H_E and H_H all equivalent and the set of four hydrogens H_B, H_C, H_F and H_G all equivalent on the NMR timescale, and so two signals due to Cp hydrogens are visible in the ^1H NMR spectra of **1–3** at ambient temperatures and above (e.g. Fig. 5).

ments of **1–3** decreases in descending order of Group IB metal congeners, as has been observed previously for a number of analogous clusters.[9–11,18]

The value of $\Delta G^{\ddagger}$ obtained for **1** is significantly larger than the ranges of *ca* 40–43 and *ca* 40–45 kJ mol^{-1}, which have been reported previously for skeletal rearrangements in the analogous clusters $[Cu_2Ru_4(\mu_3\text{-}H)_2(CO)_{12}L_2]$ (L = a variety of monodentate phosphine and phosphite ligands)[30] and $[Cu_2Ru_4(\mu_3\text{-}H)_2(\mu\text{-}L_2)(CO)_{12}]$ [$L_2 = Ph_2E(CH_2)_nPPh_2$ (E = P, n = 1, 5 and 6; E = As, n = 1 or 2) or *cis*-$Ph_2PCH{=}CHPPh_2$],[11] respectively. However, the size of $\Delta G^{\ddagger}$ measured for **1** is comparable to that of 48.1 ± 0.2 kJ mol^{-1} calculated by band-shape analysis at 298 K for the similar fluxional process in $[Cu_2Ru_4(\mu_3\text{-}H)_2\{\mu\text{-}Ph_2P(CH_2)_2PPh_2\}(CO)_{12}]$.[11] The only previously reported values of $\Delta G^{\ddagger}$ for metal core rearrangements in copper-containing clusters which are larger than that observed for **1** are 52.8 ± 0.1 (for n = 3) kJ mol^{-1}* and 52.1 ± 0.1 (for n = 4) kJ mol^{-1}* for $[Cu_2Ru_4(\mu_3\text{-}H)_2\{\mu\text{-}Ph_2P(CH_2)_nPPh_2\}(CO)_{12}]$.[11] The magnitude of $\Delta G^{\ddagger}$ for the skeletal rearrangement in the silver-containing cluster **2** is comparable to those of 40 ± 1 and 40.4 ± 0.1 kJ mol^{-1}* measured for $[Ag_2Ru_4(\mu_3\text{-}H)_2(CO)_{12}(PPh_3)_2]$[18] and $[Ag_2Ru_4(\mu_3\text{-}H)_2\{\mu\text{-}Ph_2P(CH_2)_3PPh_2\}(CO)_{12}]$,[11] respectively. It is significantly larger than the range of $\Delta G^{\ddagger}$ values of *ca* 32–36 kJ mol^{-1} observed for $[Ag_2Ru_4(\mu_3\text{-}H)_2(\mu\text{-}L_2)(CO)_{12}]$ [$L_2 = Ph_2P(CH_2)_nPPh_2$ (n = 1 or 2) or *cis*-$Ph_2PCH{=}CHPPh_2$].[11] The only previously reported values of $\Delta G^{\ddagger}$ for skeletal rearrangements in silver-containing clusters which are larger than that observed for **2** are 41.5 ± 0.1 (for n = 4)* and 42.2 ± 0.1 kJ mol^{-1}* (for n = 6)* for $[Ag_2Ru_4(\mu_3\text{-}H)_2\{\mu\text{-}Ph_2P(CH_2)_nPPh_2\}(CO)_{12}]$[11] and 45 ± 1 kJ mol^{-1} for $[Ag_2Ru_4(\mu_3\text{-}H)_2(CO)_{12}(PR_3)_2]$ (R = Pr^i or Cy).[31] Accurate quantitative comparisons of the magnitudes of $\Delta G^{\ddagger}$ for metal core rearrangements in gold-containing clusters are very difficult, since the free energies of activation are normally too small for well-resolved low-temperature NMR spectra to be obtained.[9,10,18]

The high-field hydrido ligand signals observed in the variable-temperature ^{1}H NMR spectra of **1–3** are also consistent with the clusters undergoing dynamic behaviour involving Group IB metal site-exchange within their metal skeletons, together with a concomitant site-exchange process for the hydrido ligands, at ambient temperatures in solution. At low temperatures, two signals are observed for the hydrido ligands in the ^{1}H NMR spectra of each of **1** and **2**. These two resonances are consistent with the ground-state structure of each cluster, in which the dppf ligand renders the two hydrido ligands inequivalent by removing the mirror plane through the metal skeleton [e.g. Cu(1), Cu(2), Ru(1) and Ru(4) in **1** (Fig. 3)]. For both **1** and **2**, the two ^{1}H NMR hydrido ligand signals are each split into a doublet by coupling to the phosphorus atom attached to the coinage metal which is capped by the hydrido ligands [i.e. P(1) in Fig. 1]. As expected,[13,18,31] no coupling to the other phosphorus atom [i.e. P(2) in Fig. 1] can be observed. In the case of the ^{1}H NMR spectrum of **2** at −100°C, each doublet is further split into a doublet of doublets by ^{107,109}Ag–^{1}H coupling† to the silver atom bonded to the hydrido ligands. Thus, the hydrido ligand signals observed in the low-temperature ^{1}H NMR spectra of **1** and **2** are entirely consistent with the ground-state structures of the two clusters. The value of $\Delta G^{\ddagger}$ for the intramolecular metal core rearrangement of the gold-containing cluster **3** is too small for the low-temperature limiting ^{1}H NMR spectrum to be obtained, even at −100°C, and the observed hydrido ligand signal is a singlet, which is severely broadened by the dynamic behaviour of the cluster. Unfortunately, this failure to observe the low-temperature limiting spectrum at −100°C means that it is not possible to determine the exact bonding modes of the two hydrido ligands in **3**. Both hydrido ligands could be face-capping, as they are in **1**, **2** and $[Au_2Ru_4(\mu_3\text{-}H)_2(CO)_{12}(PPr^i_3)_2]$.[32] Alternatively, one hydrido ligand could adopt a face-capping bonding mode and the other could bridge a Ru—Ru edge, as has been reported previously for $[Au_2Ru_4(\mu_3\text{-}H)(\mu\text{-}H)(CO)_{12}(PR_3)_2]$ (R = Ph[18] or Cy[32]). At ambient temperatures, a triplet is visible for the hydrido ligands in the ^{1}H NMR spectrum of each of **1** and **3**. In the case of **2**, an apparent triplet of triplets of triplets is observed. Similar patterns of signals have been reported previously for the hydrido ligands in the ^{1}H NMR spectra of silver-containing clusters analogous to **2** and analysis[13] has shown that they each consist of three superimposed subspectra, due to the three different isotopomers that are possible from the various combinations of the two naturally occurring isotopes of silver. The subspectra are each split by coupling to two chemically equivalent phosphorus atoms and those due to the ^{107}Ag^{107}Ag and ^{109}Ag^{109}Ag isotopomers are also split by couplings

* This value of $\Delta G^{\ddagger}$ was calculated at 298 K by band-shape analysis of variable-temperature ^{31}P{^{1}H} NMR spectra.

† The magnitude of the coupling between the hydrido ligands and the silver atoms is too small to allow the two separate contributions from ^{107}Ag and ^{109}Ag to be observed.

to two chemically equivalent silver atoms. Additional splittings due to ^{107}Ag–^{1}H and ^{109}Ag–^{1}H couplings are visible for the subspectrum due to the $^{107}Ag^{109}Ag$ isotopomer.

At low temperatures, eight singlets are observed for the cyclopentadienyl (Cp) hydrogens in the ^{1}H NMR spectra of **1** and **2** (e.g. Fig. 5). These two sets of signals are consistent with the ground-state structure of each cluster, in which all of the Cp hydrogens are inequivalent (Fig. 6). The value of $\Delta G^{\ddagger}$ for the skeletal rearrangement of the gold-containing cluster **3** is too low for the low-temperature limiting spectrum to be observed, even at $-100°C$. However, the peaks due to Cp hydrogens in **3** are severely broadened by the dynamic process at this temperature. At $-60°C$, four singlets due to the Cp hydrogens are visible in the ^{1}H NMR spectrum of **3**. The high-field triplet signal observed for the hydrido ligands clearly demonstrates that the intramolecular metal core rearrangement process of **3** is fast on the NMR timescale at this temperature. The four Cp peaks are consistent with this fluxional process, since each of the four inequivalent hydrogens on each Cp ring of the ligand will be exchanged with its equivalent hydrogen on the other Cp ring (i.e. the following pairs of hydrogens in Fig. 4b will be exchanged; $H_A \leftrightarrow H_H$, $H_B \leftrightarrow H_G$, $H_C \leftrightarrow H_F$ and $H_D \leftrightarrow H_E$). Four Cp hydrogen signals, which have reasonably narrow linewidths, are also observed in the ^{1}H NMR spectrum of **2** between -60 and $-50°C$ (Fig. 5). However, when the temperature is raised from -60 or $-50°C$, the four Cp peaks in the ^{1}H NMR spectra of each of **2** and **3** broaden and coalesce. At ambient temperatures and above, two resonances due to Cp hydrogens are visible for each of **2** (Fig. 5) and **3**. Clearly, the dppf ligand attached to the coinage metals in each of **2** and **3** must undergo a dynamic process which creates an effective mirror plane on the NMR timescale through both of the two C_5H_4P units. Such a process will exchange H_A with H_D and H_B with H_C on one Cp ring and H_E with H_H and H_F with H_G on the other Cp ring (Fig. 4c) and, since the two Cp rings are rendered equivalent on the NMR timescale even at $-60°C$ by the intramolecular core rearrangement, only two resonances for the Cp hydrogens would be expected at ambient temperatures. The dppf ligand in **1** must exhibit the same type of dynamic behaviour, since only two signals due to the Cp hydrogens are visible in the ^{1}H NMR spectrum of this copper-containing cluster at ambient temperatures. However, the energy barriers for the metal core rearrangement and for the dppf ligand fluxion are such that it is not possible to obtain a ^{1}H NMR spectrum showing four Cp signals with reasonably narrow linewidths (i.e. when the metal core rearrangement but not the dppf ligand fluxion is visible on the NMR timescale) at any temperature between ambient and the low-temperature limit of $-80°C$. The dynamic behaviour of the dppf ligand must involve inversion of configuration at the two phosphorus atoms and concomitant twisting of the two Cp rings. A similar fluxional process has been reported previously[16] for the dppf ligand in $[Au_2Ru_4(\mu\text{-dppf})(CO)_{12}BH]$. In the boron-containing cluster, the dppf ligand fluxion was observed to be in concert with a "rocking" motion of the two gold atoms with respect to the Ru_4B core and the two processes were found to be mutually dependent. In this context, it is interesting that the motion of the coinage metals and the fluxion of the dppf ligand are clearly not mutually dependent in **2** and **3** at least, since a ^{1}H NMR spectrum can be obtained for each cluster in which the metal core rearrangement but not the stereochemical non-rigidity of the dppf ligand is visible on the NMR timescale. In addition, it is possible that the dppf ligand in $[Ru_3(\mu\text{-dppf})(CO)_{10}]$ also exhibits the same type of fluxional behaviour as that observed for **1**–**3**. There are four distinct Cp hydrogen environments in the ground-state structure of the cluster, but the ^{1}H NMR spectrum is reported to show only two Cp multiplet signals (4H each).[17] However, the authors do not comment on the ^{1}H NMR spectrum and no information about the multiplicity of the peaks or the values of the coupling constants is given.

Dynamic behaviour involving inversion of configuration at the phosphorus atoms and twisting of the Cp rings has also been observed for dppf ligands which chelate a single metal centre.[19] Interestingly, when the dppf ligand is attached to the palladium atom in $[1\text{-}\{(dppf)Pd\}B_3H_7]$, the two fluxional processes can actually be separated and the inversion of configuration at the phosphorus atoms was found to have a higher energy barrier than that for the mutual twisting of the Cp rings.[19] Similar dynamic behaviour has also been reported[33] for [3]ferrocenophanes containing bridging main group atoms other than phosphorus.

EXPERIMENTAL

The techniques used and the instrumentation employed have been described elsewhere.[15] However, some of the ^{1}H and $^{31}P\{^{1}H\}$ NMR spectra were recorded on a Bruker AC 300 spectrometer rather than the Bruker AM 250 instrument previously cited. Light petroleum refers to that fraction of b.p. 40–60°C. Established methods were used to prepare the salt $[N(PPh_3)_2]_2[Ru_4(\mu\text{-}H)_2(CO)_{12}]$[34] and the complexes $[Cu(NCMe)_4]PF_6$[35] and

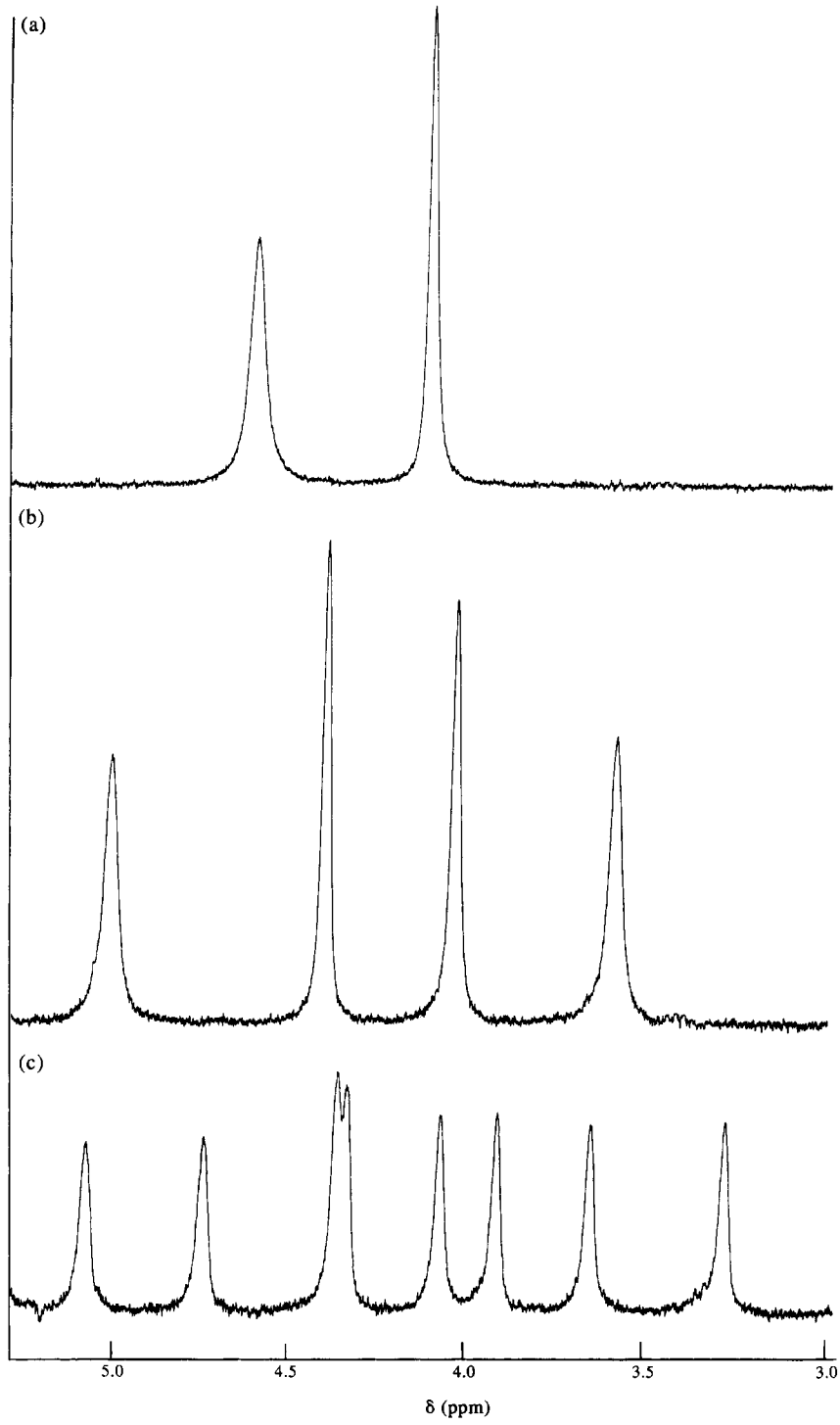

Fig. 5. The signals due to the Cp hydrogens in the ^{1}H NMR spectra of $[Ag_2Ru_4(\mu\text{-H})(\mu\text{-dppf})(CO)_{12}]$ (**2**), recorded at various temperatures. (a) The high-temperature limiting spectrum at +40°C, with both the dppf ligand fluxion and the skeletal rearrangement fast on the NMR timescale. (b) At −50°C, with the skeletal rearrangement still fast on the NMR timescale, but the dppf ligand fluxion not observed. (c) The low-temperature limiting spectrum at −100°C, when both the skeletal rearrangement and the dppf ligand fluxion are not observable on the NMR timescale.

$[AuCl(SC_4H_8)]$.[36] The compound $[Ag(NCMe)_4]PF_6$ was synthesized by an adaptation of a published route.[35,37] The ligand 1,1′-bis(diphenylphosphino)ferrocene (dppf) was synthesized by an adaptation of standard literature procedures.[38–40] Analytical and physical data for the new Group IB

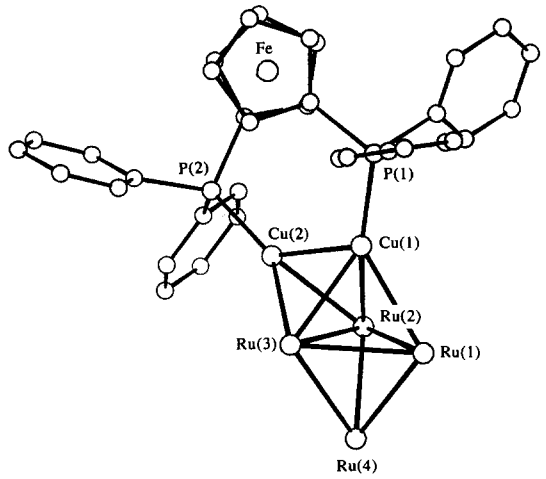

Fig. 6. A view of the relative orientations of the two C_5H_4P units in the dppf ligand attached to $[Cu_2Ru_4(\mu_3\text{-}H)_2(\mu\text{-dppf})(CO)_{12}]$ (**1**), showing that the eight hydrogen atoms bonded to carbon atoms C(2)–C(5) and C(7)–C(10) (Fig. 1) in the two cyclopentadienyl rings are all inequivalent in the ground-state structure. The hydrido and carbonyl ligands have been omitted for clarity.

metal heteronuclear cluster compounds are presented in Table 1, together with their IR spectra. Table 2 summarizes the results of NMR spectroscopic measurements. Product separation by column chromatography was performed on Aldrich Florisil (100–200 mesh) or BDH alumina (Brockman activity II).

Synthesis of $[M_2Ru_4(\mu_3\text{-}H)_2(\mu\text{-dppf})(CO)_{12}]$ (M = Cu *or* Ag)

A dichloromethane (40 cm^3) solution of $[N(PPh_3)_2]_2[Ru_4(\mu\text{-}H)_2(CO)_{12}]$ (0.60 g, 0.33 mmol) at −30°C was treated with a solution of $[M(NCMe)_4]PF_6$ (M = Cu, 0.25 g, 0.67 mmol or M = Ag, 0.28 g, 0.67 mmol) in dichloromethane (25 cm^3) and then, after stirring the reaction mixture at −30°C for 1 min, a dichloromethane (20 cm^3) solution containing dppf (0.19 g, 0.34 mmol) was added. The mixture was allowed to warm to ambient temperature with stirring and the solvent was then removed under reduced pressure. The residue was extracted with a dichloromethane–diethyl ether mixture (1 : 4; 50 cm^3 portions) until the extracts were no longer coloured red and the combined extracts were then filtered through a Celite pad (*ca* 1 × 3 cm). After removal of the solvent under reduced pressure, the crude residue was dissolved in a dichloromethane–light petroleum mixture (2 : 1) and chromatographed at −20°C on a Florisil column (*ca* 20 × 3 cm) for M = Cu or an alumina column (*ca* 20 × 3 cm) for M = Ag. In each case, elution with a dichloromethane–light petroleum mixture (2 : 1) afforded one dark red fraction which, after removal of the solvent under reduced pressure and crystallization of the residue from a dichloromethane–light petroleum mixture, yielded dark red microcrystals of the product (M = Cu, 0.28 g or M = Ag, 0.23 g).

Synthesis of $[Au_2Ru_4H_2(\mu\text{-dppf})(CO)_{12}]$ (**3**)

A dichloromethane (15 cm^3) solution of $[AuCl(SC_4H_8)]$ (0.22 g, 0.69 mmol) was treated with a dichloromethane (20 cm^3) solution of dppf (0.19 g, 0.33 mmol) and the mixture was stirred for 5 min. An acetone (40 cm^3) solution of $[N(PPh_3)_2]_2[Ru_4(\mu\text{-}H)_2(CO)_{12}]$ (0.60 g, 0.33 mmol), together with solid $TlPF_6$ (0.50 g, 1.43 mmol), was then added to the resultant solution, and the red–brown reaction mixture was stirred for 20 min. The solvent was removed under reduced pressure and the residue was extracted with a dichloromethane–diethyl ether mixture (1 : 4; 50 cm^3 portions) until the extracts were no longer coloured red. The combined extracts were then filtered through a Celite pad (*ca* 1 × 3 cm). After removal of the solvent from the filtrate under reduced pressure, the crude residue was dissolved in a dichloromethane–light petroleum mixture (2 : 1) and chromatographed on an alumina column (*ca* 20 × 3 cm). Elution with a dichloromethane–light petroleum mixture (2 : 1) afforded one red fraction which, after removal of the solvent under reduced pressure and crystallization of the residue from a dichloromethane–light petroleum mixture, yielded dark red microcrystals of the product (0.38 g).

Crystal structure determination for $[Cu_2Ru_4(\mu_3\text{-}H)_2(\mu\text{-dppf})(CO)_{12}]$ (**1**)

Suitable crystals of cluster **1** were grown from a dichloromethane–light petroleum mixture by slow layer diffusion at −20°C.

Crystal data

$C_{46}H_{30}Cu_2FeO_{12}P_2Ru_4$, $M = 1424.03$, monoclinic, space group $P2_1/n$, $a = 17.045(2)$, $b = 15.727(2)$, $c = 18.093(2)$ Å, $\beta = 94.583(2)°$, $U = 4834.62$ Å^3, $Z = 4$, $D_x = 1.956$ g cm^{-3}, $F(000) = 2768$. A red crystal of size 0.15 × 0.17 × 0.20 mm, μ(Mo-K_α) 2.36 mm^{-1}, was used for data collection.

Data collection and processing[41]

A Phillips PW1100 four-circle diffractometer was used for data collection; θ–2θ scan, 0.05° s^{-1}, $2\theta_{max} = 50°$ for the range $-20 \leqslant h \leqslant 19$, $0 \leqslant k \leqslant 18, 0 \leqslant l \leqslant 21$; three reflections monitored every 200 min with no significant variation. Equivalent reflections were averaged to give 4220 unique data with $I/\sigma(I) > 3.0$. Corrections were made for Lorentz polarization factors, and absorption corrections were applied to the data after initial refinement of the isotropic thermal parameters of all the non-hydrogen atoms.[42]

Structure solution and refinement

The position of the metal atoms defining the capped trigonal bipyramidal metal core structure in **1** were obtained from a Patterson synthesis. The remaining non-hydrogen atoms were found from subsequent Fourier-difference syntheses.[43] Although the two hydrido ligands in the structure of **1** were not located directly from the data, suitable positions were obtained from potential energy minimization calculations.[44] These atoms were included in the structure factor calculations, with fixed thermal parameters of 0.08 Å^2, but their parameters were not refined. The carbon atoms of the phenyl and the cyclopentadienyl rings were grouped together as rigid hexagons [d(C—C) = 1.395 Å] and pentagons [d(C—C) 1.420 Å], respectively. The hydrogen atoms were included in geometrically idealized positions and constrained to "ride" on the relevant carbon atoms [d(C—H) = 1.08 Å] with common group isotropic thermal parameters of 0.08 Å^2, which were not refined. Anisotropic thermal parameters were assigned to the metal and the phosphorus atoms during the final cycles of full-matrix refinement which converged at R and R' values of 0.0513 and 0.0509, with weights of $w = 1/\sigma^2(F_o)$ assigned to individual reflections.

Acknowledgements—We thank Exeter University for a studentship (S. A. W.), Johnson Matthey plc for a generous loan of gold, silver and ruthenium salts, Mr Roger Lovell for technical assistance, Mr Graham Luscombe for producing Figs 2 and 4a and the structural formulae, and Dr Peter Heard for producing Fig. 4b and c.

REFERENCES

1. Part 17. P. J. McCarthy, I. D. Salter and T. Adatia, *J. Organomet. Chem.* 1995, **485**, 191.
2. D. G. Evans and D. M. P. Mingos, *J. Organomet. Chem.* 1982, **232**, 171.
3. D. J. Wales, D. M. P. Mingos and L. Zhenyang, *Inorg. Chem.* 1989, **28**, 2754.
4. D. M. P. Mingos, *Polyhedron* 1984, **3**, 1289.
5. I. D. Salter, *Adv. Dynamic Stereochem.* 1988, **2**, 57.
6. I. D. Salter, *Adv. Organomet. Chem.* 1989, **29**, 249.
7. D. M. P. Mingos and M. J. Watson, *Adv. Inorg. Chem.* 1992, **39**, 327.
8. I. D. Salter, in *Comprehensive Organometallic Chemistry* II (Edited by G. Wilkinson, F. G. A. Stone and E. W. Abel), Vol. 10. Pergamon, Oxford (1995, in press).
9. S. S. D. Brown, I. D. Salter, A. J. Dent, G. F. M. Kitchen, A. G. Orpen, P. A. Bates and M. B. Hursthouse, *J. Chem. Soc., Dalton Trans.* 1989, 1227.
10. S. S. D. Brown, I. D. Salter, D. B. Dyson, R. V. Parish, P. A. Bates and M. B. Hursthouse, *J. Chem. Soc., Dalton Trans.* 1988, 1795.
11. C. P. Blaxill, S. S. D. Brown, J. C. Frankland, I. D. Salter and V. Šik, *J. Chem. Soc., Dalton Trans.* 1989, 2039.
12. T. Adatia, *Acta Crystallogr.* 1993, **C49**, 1926.
13. S. S. D. Brown, I. D. Salter and L. Toupet, *J. Chem. Soc., Dalton Trans.* 1988, 757.
14. S. S. D. Brown, I. D. Salter, V. Šik, I. J. Colquhoun, W. McFarlane, P. A. Bates, M. B. Hursthouse and M. Murray, *J. Chem. Soc., Dalton Trans.* 1988, 2177.
15. S. S. D. Brown, P. J. McCarthy, I. D. Salter, P. A. Bates, M. B. Hursthouse, I. J. Colquhoun, W. McFarlane and M. Murray, *J. Chem. Soc., Dalton Trans.* 1988, 2787.
16. S. M. Draper, C. E. Housecroft and A. L. Rheingold, *J. Organomet. Chem.* 1992, **435**, 9.
17. S. T. Chacon, W. R. Cullen, M. I. Bruce, O. bin Shawkataly, F. W. B. Einstein, R. H. Jones and A. C. Willis, *Can. J. Chem.* 1990, **68**, 2001.
18. M. J. Freeman, A. G. Orpen and I. D. Salter, *J. Chem. Soc., Dalton Trans.* 1987, 379.
19. For example, C. E. Housecroft, S. M. Owen, P. R. Raithby and B. A. M. Shaylih, *Organometallics* 1990, **9**, 1619 and references cited therein.
20. M. Müller-Glieman, S. V. Hoskins, A. G. Orpen, A. L. Ratermann and F. G. A. Stone, *Polyhedron* 1986, **5**, 791.
21. H. Deng and S. G. Shore, *Organometallics* 1991, **10**, 3486.
22. H. Hartung, B. Walther, U. Baumeister, H.-C. Böttcher, A. Krug, F. Rosche and P. G. Jones, *Polyhedron* 1992, **11**, 1563.
23. B. F. G. Johnson, J. Lewis, W. J. H. Nelson, M. D. Vargas, D. Braga, K. Henrick and M. McPartlin, *J. Chem. Soc., Dalton Trans.* 1986, 975.
24. J. S. Bradley, R. L. Pruett, G. B. Ansell, M. E. Leonowicz and M. A. Modrick, *Organometallics* 1982, **1**, 748.
25. P. Braunstein, J. Rosé, A. Dedieu, Y. Dusausoy, J. P. Mangeot, A. Tiripicchio and M. Tiripicchio-Camellini, *J. Chem. Soc., Dalton Trans.* 1986, 225.
26. A. Fumagalli, S. Martinengo, V. G. Albano and D. Braga, *J. Chem. Soc., Dalton Trans.* 1988, 1237.
27. C. E. Housecroft, S. M. Owen and P. R. Raithby, unpublished results; cited in B. F. G. Johnson, R. Khattar, J. Lewis and P. R. Raithby, *J. Chem. Soc., Dalton Trans.* 1989, 1421.

28. S. S. D. Brown, S. Hudson, I. D. Salter and M. McPartlin, *J. Chem. Soc., Dalton Trans.* 1987, 1967.
29. R. A. Brice, S. C. Pearse, I. D. Salter and K. Henrick, *J. Chem. Soc., Dalton Trans.* 1986, 2181.
30. G. V. Goeden and K. Caulton, *J. Am. Chem. Soc.* 1981, **103**, 7354.
31. P. J. McCarthy, I. D. Salter, and V. Šik, *J. Organomet. Chem.* 1988, **344**, 411.
32. C. J. Brown, P. J. McCarthy and I. D. Salter, *J. Chem. Soc., Dalton Trans.* 1990, 3583.
33. For example, E. W. Abel, M. Booth and K. G. Orrell, *J. Organomet. Chem.* 1981, **208**, 213 and references cited therein.
34. S. S. D. Brown and I. D. Salter, *Organomet. Synth.* 1988, **4**, 241.
35. G. J. Kubas, *Inorg. Synth.* 1979, **19**, 90.
36. R. Uson and A. Laguna, *Organomet. Synth.* 1986, **3**, 324.
37. S. S. D. Brown and I. D. Salter, *Organomet. Synth.* 1986, **3**, 315.
38. G. Marr and T. Hunt, *J. Chem. Soc.* (*C*) 1969, 1070.
39. J. J. Bishop, A. Davison, M. L. Katcher, D. W. Lightenberg, R. E. Merrill and J. C. Smart, *J. Organomet. Chem.* 1971, **27**, 241.
40. W. R. Cullen, R. W. B. Einstein and T. Jones, *Organometallics* 1983, **2**, 714.
41. M. K. Cooper, P. J. Guerney and M. McPartlin, *J. Chem. Soc., Dalton Trans.* 1982, 757.
42. N. Walker and D. Stuart, *Acta Crystallogr.* 1983, **A39**, 158.
43. G. M. Sheldrick, *SHELX 76*, Program for Crystal Structure Determination, University of Cambridge (1976).
44. A. G. Orpen, *J. Chem. Soc., Dalton Trans.* 1980, 2509.